Progress and challenges of the ECH transmission line design for DTT

Fusion Engineering and Design 202 (2024) 114391

Contents lists available at ScienceDirect

Fusion Engineering and Design

journal homepage: www.elsevier.com/locate/fusengdes

Progress and challenges of the ECH transmission line design for DTT

A. Moro [a,*], A. Bruschi [a], F. Fanale [b,c], P. Fanelli [d], E. Gajetti [e], S. Garavaglia [a], G. Granucci [a], S. Meloni [d], A. Pepato [f], P. Platania [a], A. Romano [b,c], A. Salvitti [d], L. Savoldi [e], S. Schmuck [a], M. Scungio [d], A. Simonetto [a], M. Turcato [f], E. Vassallo [a]

[a] Institute for Plasma Science and Technology (ISTP-CNR), Italy
[b] ENEA, Fusion and Nuclear Safety Department, C.R. Frascati, Frascati, Italy
[c] DTT S.C. a r.l., Via E. Fermi 45, I-00044, Frascati (RM), Italy
[d] Department of Economics, Engineering, Society and Business Organization, Tuscia University, Viterbo, Italy
[e] Energy Department 'Galileo Ferraris', Politecnico di Torino, Italy
[f] National Institute for Nuclear Physics, INFN Padova Division, Italy

ARTICLE INFO

Keywords:
Electron cyclotron heating
Transmission line
Electromagnetic simulations
Aberrations

ABSTRACT

The design of the Transmission Line (TL) as a part of the Electron Cyclotron Heating (ECH) system for Divertor Tokamak Test facility (DTT) is approaching the conceptual design maturity. With an ECH system of 16 MW installed for the first phase and with a total of 32 gyrotrons (170 GHz, ≥ 1 MW, 100 s) the TL design is undertaking the challenge of an evacuated Multi-Beam TL (MBTL) concept to deliver the large number of beam lines from the gyrotron hall to the torus hall buildings. The system is organized in 4 clusters, each of them including 8 beamlines. The routing consists of single-beam TL section used to connect the gyrotron output to a beam-combiner mirror unit for each cluster, a common MBTL running in a suspended corridor reaching the Tokamak building and a beam-splitter mirror unit to connect to the ex-vessel optics and launchers sections located in the equatorial and upper ports of one sector, for a total of 4 DTT sectors. The TL mirrors will be actively water cooled to cope with the heat load in long pulses due to the high power incident radiation, with the possibility to include advanced concepts for the cooling design compatible with additive manufacturing technology. The characteristics of the system and its components are presented, showing both the progress of the adopted solutions and the current design. Since the main challenge of this TL is to maintain the overall losses below 15%, in this paper we present the expected ohmic and spillover losses, including beam coupling simulations evaluating losses given by high order Transverse Electro-Magnetic modes (i.e. aberrations). We describe how the effects have been estimated with electromagnetic simulations and how losses could be mitigated, since TL efficiency could significantly drop due to the presence of non-idealities, like the deformations of mirrors surface ascribed to the microwaves heat loads and possible misalignments and aberrations effects occurring along the line.

1. Introduction

The power exhaust problem in an integrated environment and DEMO-relevant conditions will be addressed in the DTT (Divertor Tokamak Test) facility [1]. To pursue this, the Tokamak device will rely on 45 MW to the plasma from external heating systems, provided by Electron Cyclotron Heating (ECH) [2], Ion Cyclotron Heating and Neutral Beam Injection, installed in three different phases. For the first phase of DTT operations the installed power of the ECH system will consist of 16 MW, operating at 170 GHz and equipped with 16 gyrotron units (≥1 MW, 100 s). Additional 16 MW of ECH with the same or higher power are planned in later phases of DTT operations, to reach at least 32 MW of ECH installed power. The entire system is organized in 4 clusters, with 8 gyrotron units per cluster. The Transmission Line (TL) delivering the radio frequency power from the gyrotron hall to the torus hall building incorporates an evacuated Multi-Beam TL (MBTL) [3] where 8 beam-lines propagate sharing optical elements designed with confocal configuration to reproduce quasi-optical beams after long distance. The entire TL is enclosed in evacuated pipes (with a pumping system providing 10^{-3} Pa pressure to reduce risk of arcs) and combining single lines into multi-beam lines consisting of large plane and parabolic mirrors. Active water-cooling is also foreseen to mitigate deformations of the mirrors surface that otherwise would alter the transmission efficiency of

* Corresponding author.
E-mail address: alessandro.moro@istp.cnr.it (A. Moro).

https://doi.org/10.1016/j.fusengdes.2024.114391
Received 16 October 2023; Received in revised form 10 March 2024; Accepted 22 March 2024
Available online 5 April 2024

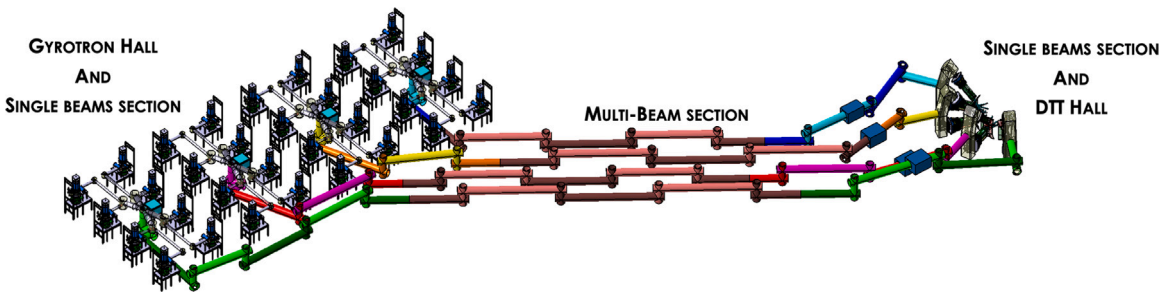

Fig. 1. The three sections and four Clusters of the ECH system of DTT. Single-Beam section in the Gyrotron hall with beam combiner at interface, the Multi-Beam section (with 17-17-21-25 mirrors for the four Clusters) and the Single-Beam section connecting to DTT torus hall (with beam splitter at the interface).

the line. At the end of the TL two front-steering antennas, located in the equatorial and upper ports [4] will inject the beams into the vacuum vessel and ultimately into DTT plasma. The concept of TL exploiting single-beams and multi-beams sections has been successfully developed and is presently operating in W7-X stellarator [5,6], an exclusively quasi-optical open-air transmission line from which the DTT TL design drew inspiration.

2. Transmission line design and mm-waves characterization

The design of TL routing consists of three sections, connecting the Gyrotron Hall building and the torus Hall and coping with planimetry and engineering constraint at DTT site: a Single-Beam section in the Gyrotron hall (SBG), where the beams from the gyrotrons propagate with independent optical path, a Multi-Beam section (MB) where the eight beams of a given cluster are grouped in a single optical path and a final Single-Beam section where the bundle of beams is splitted into independent optical paths towards the dedicate DTT sectors hosting the ECH launchers (SBD). A combiner and a splitter mirror units act as optical interface connections between the aforementioned sections. Fig. 1 shows the model of the ECH system with its different sections. The TL is enclosed in evacuated pipes and operating at pressures such that risk of breakdown according to Paschen's curve is avoided [7]. From the optical point of view the MB section exploits the confocal configuration, combined with doglegs and alternating shaping and plane mirrors. Considering the large number of mirrors this is optimal to replicate a given input field distribution after long distances like the ones foreseen in the ECH system of DTT where the entire TL length ranges from 84 m for the shortest case (Cluster I) to 137 m for the longest case (Cluster IV).

The complete quasi-optical system has been implemented into the commercial code GRASP [8], which is used to characterize and validate the optics and the resulting mm-wave propagation. In this work we present results of electromagnetic simulations done for Phase 1 Clusters (I and II) due to the higher priority for first plasma operations. The GRASP model has been used to evaluate spill-over losses of the TL, considering the finite dimensions of the reflecting surfaces and propagating beams. The technique adopted in these simulations is Physical Optics (PO), supplemented with the Physical Theory of Diffraction (PTD). Examples of TL sections modelled can be seen in Figs. 2 and 3, where the regions at the combiner and splitter interfaces are shown: in Fig. 2 it can be seen how 4 out 8 single-beam sections (smaller mirrors) reach the combiner mirror to be injected in the multi-beam section (larger mirrors), while Fig. 3 shows how last mirrors of the multi-beam section direct the 8 beams of the cluster towards the splitter unit to separate the beam-lines back to single ones and aiming at the final section of the TL and reaching the ECH ports located in DTT Hall.

The relative power hitting scatterer n (P_n) is defined as the power incident on the scatterer $P_{in,n}$ normalized to the gyrotron power P_G: $P_n = P_{in,n}/P_G$. The spillover loss L_n at mirror M_n is defined as the difference

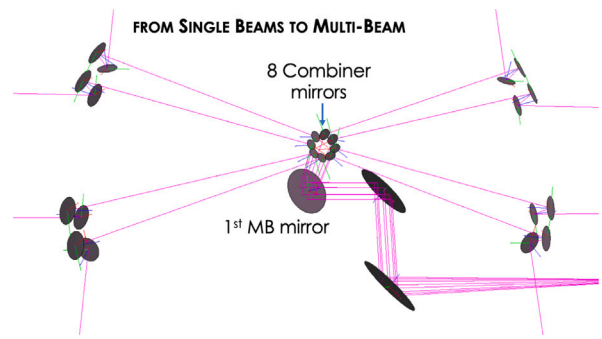

Fig. 2. Graphical GRASP representation of quasi optical system sections. In the Gyrotron hall the eight Single-Beams are combined and directed towards the MB section (larger mirrors).

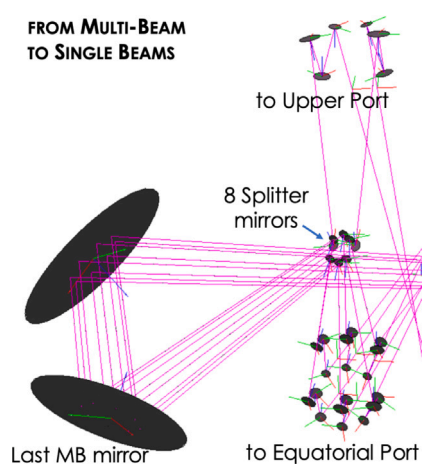

Fig. 3. Graphical GRASP representation of quasi optical system sections. After the last MB mirror the beams are splitted again into eight Single-Beams to be directed towards the DTT hall.

between the relative power P_{n-1} hitting mirror M_{n-1} and that hitting mirror M_n:

$$L_n = (P_{n-1} - P_n) \tag{1}$$

L_n thus represents power leaving the optical system between mirrors M_{n-1} and M_n. For the last mirror N, P_n is the relative power reflected by the mirror, accounting spillover losses of all the preceding reflections. We consider the spillover loss along the TL as the source of stray radiation. Table 1 summarizes the power fraction P_N hitting the last scatterer, while Fig. 4 presents for Clusters I (left) and II (right) the values the power fraction hitting each mirror (planar or shaping) for the 8 beams respectively (the labels from #1 to #8 are used for simplicity to identify the beam of a given cluster). It can be seen how the transition

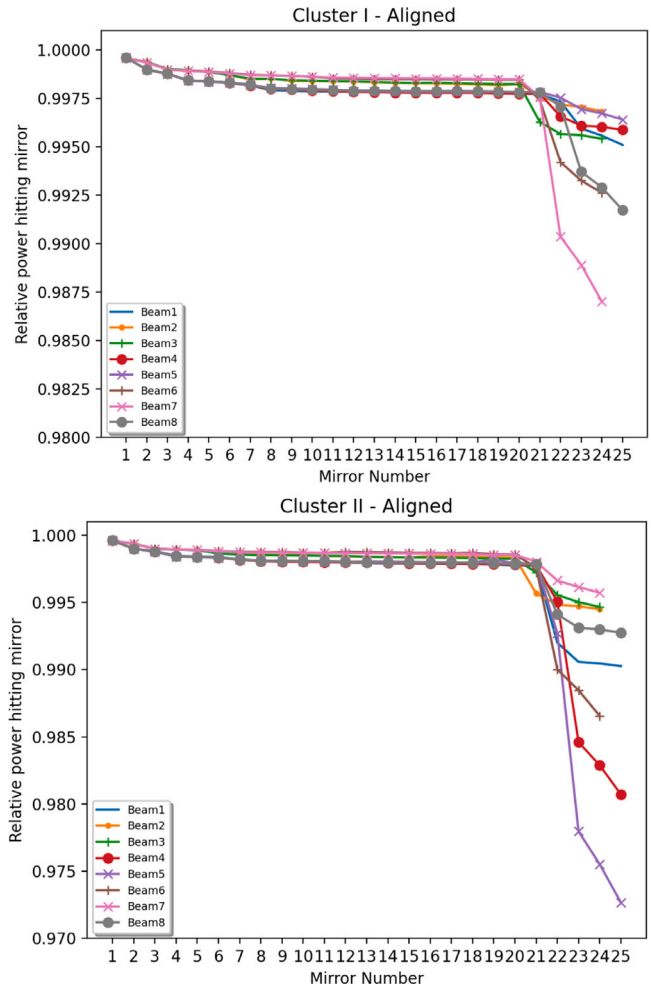

Fig. 4. Power fraction hitting the mirrors of Clusters I (top) and II (bottom) for the eight beams along the full transmission line.

Table 1
Relative power hitting the last scatterer.

Beam label	Cluster I rel. pow.	Cluster II rel. pow.
#1	0.9951	0.9903
#2	0.9968	0.9945
#3	0.9954	0.9947
#4	0.9959	0.9807
#5	0.9964	0.9723
#6	0.9926	0.9866
#7	0.9970	0.9957
#8	0.9917	0.9927

from MB to the final single-beam section results in an increased spill-over, due to the constraints in the routing adaptation after the splitter mirrors unit that introduces aberrations. We ascribe the difference between the values for the two clusters (mean values 0.6% and 1.2% over the eight beams of Clusters I and II respectively) to the different routing geometry in the last section of the MB and from the splitter units to the DTT sectors.

A further outcome from spillover analysis is the possibility to evaluate the amount of stray radiation at a given location along the TL, to identify risks of over-heating in specific regions. At the location of the eight splitters for instance, the expected stray power is up to 37.7 kW summing up the values for the eight beams contribution, occupying the volume that will host the mirrors and that requires to be dissipated. Further up along the SBD section towards DTT ports, despite single beam-lines have mirrors with higher fraction of lost power, we do not expect values higher than 10.9 kW, with no contribution from nearby beam-lines.

Table 2
Mean value of HOTMs content [%] for the 8 beams of Cluster II in the TL sections.

HOTMs content [%]	SBG	MB	SBD	TL
	0.25	4.82	0.25	5.35

The electromagnetic simulations also provide the contribution to the TL losses due to the spurious modes content generated along the propagation. Considering an ideal Gaussian beam (100% TEM_{00} content) at the gyrotron port, the coupling to TEM_{00} at the launcher waveguide opening is 90.3–98.3%, i.e. the spurious *TEM* mode content is in the range [1.7%–9.7%] in case of Cluster II. In order to evaluate the amount of transmitted power, regardless the *TEM* mode mixture, we computed the spill-over loss at the transition from QO propagation to the waveguide propagation segment, occurring at the interface with the ECH launchers. With 63.5 mm diameter corrugated waveguide, the fractional power not entering the waveguide is found in the range [2.8%-4.3%] for the eight beams of Cluster II.

Table 2 shows the fraction of Higher Order *TEM* Modes (HOTMs) as resulting from the electromagnetic simulation along the TL in the three sections of the system, computed independently. SBG is the Single-Beam section in the Gyrotron hall, MB is the Multi-Beam section of the TL, SBD the Single-Beam section in the DTT hall and TL the complete TL from gyrotron matching optics unit window to ECH ports. The MBTL contribution is dominating, considering the number of mirrors and routing. The presence of HOTMs in the propagating beam will result in a reduction of the power coupled to the main TEM_{00} mode, with larger contributions from higher order modes. Fig. 5 shows the quantity $|E|^2$ evaluated at the QO transition for the best (top) and worst (bottom) beams of Cluster II in terms of spurious mode content. The power density (rate of energy transfer per unit area) is the product of the electric field E times the magnetic field H and proportional to $|E|^2$ in the far field. What has to be noted is how the −8.7 dB black contour level, equivalent to the Gaussian Beam radius is not matching the design value (20.43 mm, red curve) for the worst beam, as found in the case of Beam 3. The white circle is added to mark the 63.5 mm waveguide diameter.

Another important source of losses in QO systems is given by the ohmic losses occurring on metallic surfaces, represented in our case by copper mirrors. We could evaluate the amount of these losses considering the electrical properties of pure copper (using $\rho = 1.74$ Ω m at 20 °C for copper resistivity to compute surface resistance R_s), a roughness factor 1.3 [3] and the effect of wave polarization along the transmission line. It is well known how the field components parallel and perpendicular to the plane of incidence determine the lost power fraction with respect to the incident one, considering the power reflection coefficients [9]

$$r_{\parallel}^2 = 1 - 4\frac{R_s}{Z_0}\frac{1}{\cos\theta} \tag{2}$$

$$r_{\perp}^2 = 1 - 4\cos\theta\frac{R_s}{Z_0} \tag{3}$$

and according to the following equation:

$$\frac{P_{loss}}{P_0} = 1 - \prod_1^M \left(\frac{E_{\parallel}^2}{E_0^2}\left(1 - 4\frac{R_s}{Z_0}\frac{1}{\cos\theta}\right) + \frac{E_{\perp}^2}{E_0^2}\left(1 - 4\frac{R_s}{Z_0}\cos\theta\right)\right) \tag{4}$$

where P_{loss}/P_0 is the lost power fraction, M the number of mirrors of the TL, $E_{\perp}/E_0$ and $E_{\parallel}/E_0$ the normalized components of the E field in the plane of incidence and orthogonal to the plane of incidence respectively, $Z_0 = 376.73$ Ω the impedance of free space and θ the incidence angle. The physics requirements for the ECH system call for the inclusion of a universal polarizer system in the SBD section, made by two $\lambda/8$ mirror for each beam line. The possibility to add a linear

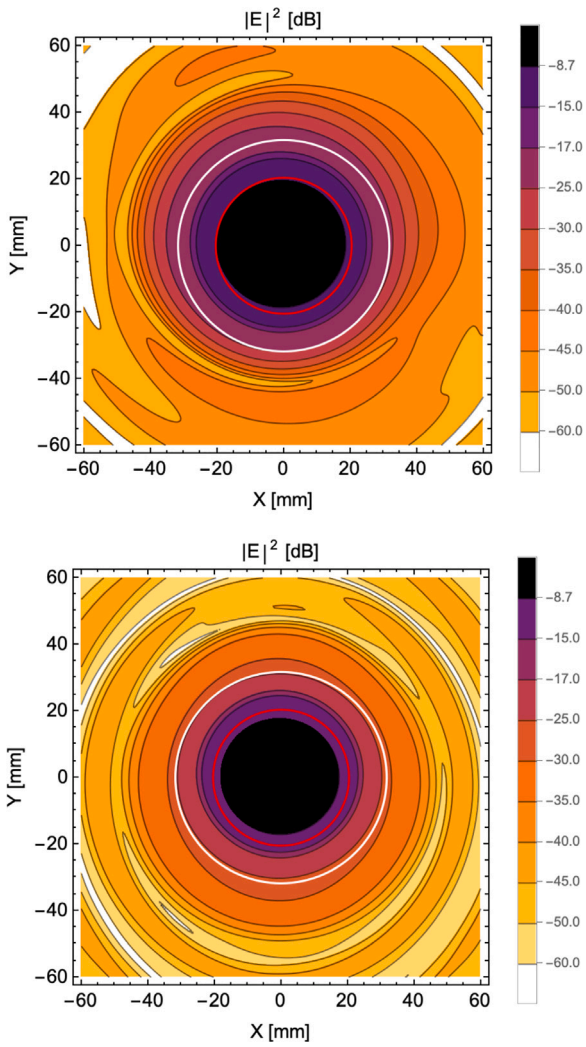

Fig. 5. $|E^2|$ for lowest (top) and highest (bottom) High Order TEM Modes content for Cluster II beams at the QO/WG interface. The red circle represents the contour of the beam radius design value (−8.7 dB), the white circle the 63.5 mm QO/WG transition diameter.

polarizer before the MB, in order to optimize the polarization along the section, is still under discussion and we are now considering thus the universal polarizer only. The rationale for the choice of a pair of $\lambda/8$ mirrors as universal polarizers instead of a pair $\lambda/4$-$\lambda/8$ is justified by the promising results found in [10]. Such a configuration has lower losses and provides cost benefits, since only one type of grooved mirror needs to be manufactured. In order to sum up all the contributions and estimate the TL losses, we need to consider the interface between the single-beam section in the DTT hall and the ports hosting the launchers, where a wave-guide section has been introduced after the last mirror of the SBD and the first mirror in the antenna. A Quasi-Optical/Wave Guide/Quasi-Optical (QO/WG/QO) transition is thus considered, with WG diameter 63.5 mm. The length of the WG section and the ratio be of beam radius w to WG inner radius a can be chosen to approach the optimum TEM_{00} to HE_{11}-HE_{12} power coupling, given by 99.85% for w/a = 0.5 according to [11] and L_{WG} = 1827 mm (corresponding to HE_{11}-HE_{12} beat-length, which is one of the options discussed in [4]). With a minimum combination of adjustments of the focal lengths of the last shaping mirror of the single-beam lines and of the shaping mirror of the ECH launcher, ≈0.5% coupling loss can be achieved, as resulting from simulations obtained with TEM_{00} as source at the waveguide (simulations taking into account the output of the TL are beyond the scope of this paper). This also taking into account expected low value for waveguide ohmic losses, according to the model described in [12], adapted to our case and considering different material options, respectively 0.003% and 0.02% for stainless steel and copper.

Table 3
TL losses contributions [%] in the ideal case.

Cluster	I	II
Ohmic (SBG+MB+SBD)	4.7	4.6
Spillover at DTT port	2.8	4.3
QO/WG/QO transition	0.5	0.5
Total	8.0	9.4

Table 3 summarizes the TL total losses when contribution from Ohmic, spillover and QO/WG/QO transition losses are considered. The value of the spillover is here evaluated at the entrance of the waveguide section in proximity of the DTT port. We see that in the ideal case, with no additional effects from deformations and misalignments included, the value is <10% for Clusters I and II. The following Sections will describe how those effects will be included in the analysis.

3. Mirrors deformation effects

To evaluate the effects of mirrors deformation on beam propagation along the TL, the heat loads on the mirrors have been determined. Different options for the cooling system layout are being considered and include spiral channels embedded in the bulk of the mirrors of the MB section (2 cm Cu bulk, 4 mm Cu layer, 1.2–1.5 cm channel diameter, with 8 beams and 1 MW per beam) determining the incident heat load. For the mirrors of the single-beam sections (1 MW per beam) spiral channels and Triply-Periodic Minimal Surfaces (TPMS) for the most loaded TL mirrors, namely the combiner, the splitter and the polarizers are investigated.

The effects of the heat load on cooled MB mirror could be evaluated considering 8 Gaussian distributions of the incident power, corresponding to the single beam profiles distributed over the mirrors surface according to the (ideal) optical configuration. The different loads reflect the possible cases of parabolic mirror, flat mirror in the path with parallel propagating beams and flat mirror with beams propagating from/to a focal point. An example of the system designed for a large flat mirror is shown in Fig. 6 (left), paired to the expected heat load due to the 8 beams Fig. 6 (right). The heat load distributions, with a less loaded area in the central region of the mirror drove an option for the cooling design using one inlet and two outlets, with the inlet split in two symmetric channels to provide uniform cooling over the surface. When the water cooling system parameter are taken into account (20 l/min, inlet water temperature T_{in} = 15 °C), thermo-mechanical analyses [13] provided the modified mirror surface, with maximum deformation = 0.1 mm in this case (T_{max} = 28.7 °C). Other mirrors have been similarly studied, as can be found in [14], where more details on the method and models are described. The TEM_{00} to TEM_{00} Gaussian beam coupling in a modular unit of the MB (8 mirrors in total considered) has been calculated with GRASP for representative beams and the values compared to the coupling in the case of unperturbed mirrors surfaces. The results show that the fraction of spurious mode in a modular MB unit increases by a factor 3.5 (from 0.16% in the case of undeformed mirror to 0.56% when the 8 deformed surfaces are taken into account). Mitigation of the deformation effects is thus required for MB mirrors, to reduce the spurious mode content that would be unacceptably high when the effect of all the 17 mirrors of the MB will be simulated. In the present configuration, a maximum mirror deformation in the range 0.08–0.12 mm has been found at the end of 100 s pulse, resulting in offset of the reflection points along the MBTL mirrors up to 3 cm. As a consequence of this, the total spillover loss at the end of the line rises up to 7.4% for Cluster II. This value, when compared to the one found in the undeformed case, would give total losses of the line >10% that we are presently considering as maximum losses limit.

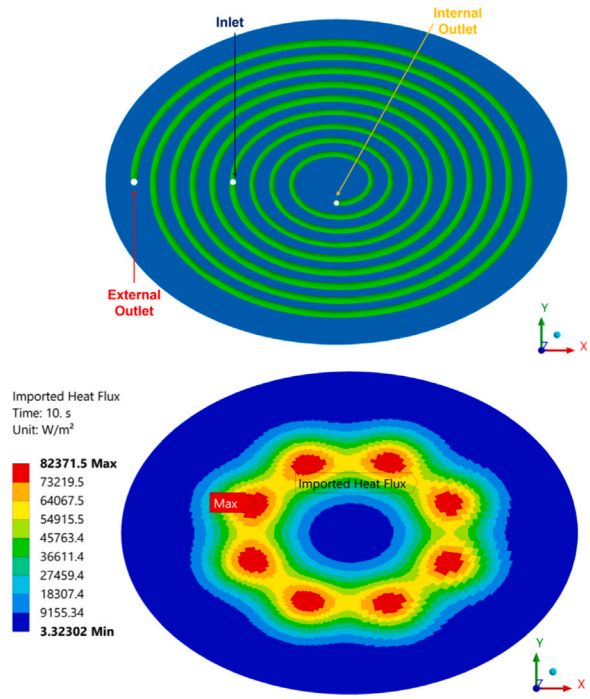

Fig. 6. Left: Model of the presently proposed cooling channel for a mirror of the MBTL. The inlet splits in two symmetric channels to provide uniform cooling over the surface and ending up in two outlets, one internal and one located at the outer part of the mirror. Right: heat load considering bi-dimensional Gaussian distributions for the 8 propagating beams. The absorbed power is then evaluated in the case of a copper mirror.

Similar analysis has been performed for a reduced set of SB mirrors, showing better results in terms of surface deformation. Despite one beam only is reflected off these mirrors, the peak power density due to the beam spot size might be relevant, requiring the development of novel concepts for the cooling system, like the TPMS. The geometry of these structures is determined by 3D sine/cosine functions generating non-self-intersecting structures that are used to enhance the heat transfer due to high surface-to-volume ratio and low weight [15]. These structures are becoming more popular also because their manufacture has been allowed by the boost of additive manufacturing. Their excellent performance as heat sinks has been recently demonstrated by numerical investigations in [16] and is here considered for the splitter and combiner mirrors of the TL, where the highest heat load in terms of peak power density P_0 = 1.6 MW/m^2. Fig. 7, taken from [17], shows how TPMS have been modelled and implemented in the splitter mirror design (reddish brown image), considering 4 × 4 × 4 mm^3 unit cells (grey image). Taking into account again the water cooling system parameters (4.2 l/min, inlet water temperature T_{in} = 15 °C), thermo-hydraulic and thermo-mechanical simulations provide maximum deviations from the nominal condition of 5.6 10^{-5} m (T_{max} = 32.5 °C) and $P_0/\Delta T_{max}$ = 79.6 MW m^2 K^{-1}, which could represents a figure of merit, since large values of the ratio $P_0/\Delta T_{max}$ are beneficial. In the case of shaping mirrors and investigating for them the spiral cooling channels option, we obtain a maximum deformation of the order of 2 10^{-5} m with mirror T_{max} = 27.0 °C, values that are lower than the splitter case. It has although to be noted that for this mirror $P_0/\Delta T_{max}$ = 19.5 MW m^2 K^{-1}. Electromagnetic simulations to evaluate the effect of these deformations on spurious mode content and beam propagation are planned to complete the analysis on TL mirrors.

4. Misalignments preliminary study

Assessing the required tolerance in the alignment of mirrors is essential for specifying supports and installation procedures. A Monte-Carlo analysis of the geometric optics path of the central ray of each

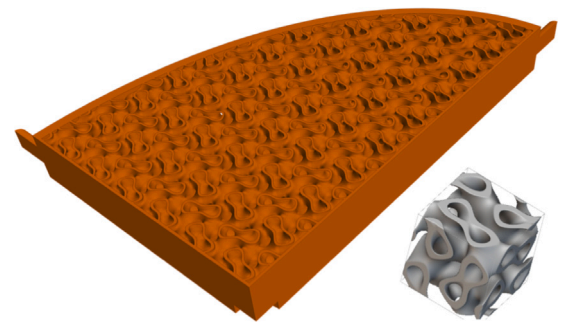

Fig. 7. Computational domain of the mirror equipped with TPMS cooling structure. The top heated wall in the reddish brown image has been removed here for the sake of clarity, while the grey image represent the single TPMS unit cell.

beam has started aiming at the identification of preliminary alignment tolerance for a given mirror. A Fortran program [18] is used to simulate perturbations in mirrors orientation with a uniform distribution function within specific tolerances for optical systems characterized by a sequence of flat and conic surfaces. The program is able to allow a large number of random perturbations. The moments of the probability distribution obtained are used to quantify its main characteristics. The nth-order moments are computed for beam axis position and orientation at each mirror. In particular the 2nd order momentum

$$M_2(\Delta w) = \frac{1}{N}\sum_{i,j}[\Delta w(i,j)]^2 \tag{5}$$

represents the variance of the distribution, where N is the total number of random cases and $\Delta w(i,j)$ is the distance between the unperturbed quantity and the i,jth instance of the perturbation. The perturbed quantities considered are angle of reflection and point of incidence of the central ray. In both cases, separate values are computed for displacements in the unperturbed plane of incidence and across it. The square root of M_2, corresponding to the standard deviation of the distribution, is used as an indicator of the misalignment (angular or linear) on a given mirror in the perturbed case. Fig. 8 shows results as a function of the mirror number (#elem) in the case of beam #1 of Cluster I, using different tolerances for SB (10^{-3} rad) and MB (10^{-4} rad) mirrors, corresponding to 1 mm/m and 0.1 mm/m respectively, for 10^4 cases. It has to be noted how linear displacements of the order few mm are found at TL end, displacements <2.0 cm might have to be recovered along the MB section. These displacements can be reduced either requiring more stringent tolerances in the design and construction phase or considering the possibility to recover TL alignment with actuators and control system, which is the option presently under investigations but out of the scope of this paper.

A case of accidental misalignment, not randomly generated, has been investigated evaluating the effects of the wind blowing on the elevated (14 m high), stiffened corridor hosting part of the MB section. Considering a medium intensity wind (8 m/s speed) and given the building movements, we could set displaced MB mirrors, under the assumption of linearly increasing displacement from the fixed nodes (in proximity of DTT hall) to the most displaced ones (in proximity of the gyrotron hall), up to 0.7 mm horizontal displacement. As a result of simple ray-tracing simulations we could find that, with respect of the aligned case, the expected linear beam displacement at QO-WG interface is 0.4 mm, at the location of the beam splitter 0.8 mm, and linear displacements in the MB section up to 1.7 mm. In terms of spillover loss, this additional contribution is not significant (<0.1%) and does not affect the overall TL losses determined in Section 2.

5. Conclusions

The design of the Transmission Line as a part of the Electron Cyclotron Heating system for Divertor Tokamak Test facility is approaching the conceptual design maturity. It undertakes the challenge

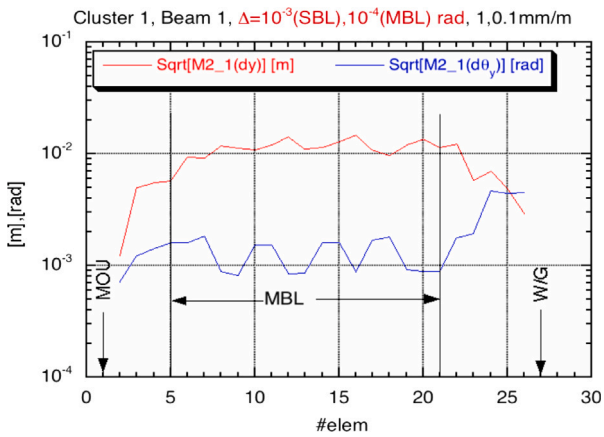

Fig. 8. Square root of the 2nd order momentum of the distribution for linear (dy) and angular (dθ) displacements when random perturbations along the TL of Cluster I are simulated with different tolerances for SB and MB sections.

of an evacuated Multi-Beam transmission line concept to deliver the large number of beam lines from the gyrotron hall to the torus hall buildings. The characteristics of the system are presented, showing both the progress of the adopted solutions and the current design. The ohmic losses, spill-over and beam coupling simulations for the nominal case and the main expected sources of non idealities are outlined. Methods and tools to evaluate how those sources would affect the transmission line losses, lower than 10% in the ideal case, have been also presented. Further analysis of the effects of mirrors deformation and misalignment investigations will drive the design of the transmission line in the next phase, in order to assess or review the concepts developed so far.

CRediT authorship contribution statement

A. Moro: Writing – review & editing, Writing – original draft, Supervision, Investigation, Funding acquisition. **A. Bruschi:** Software, Methodology, Investigation. **F. Fanale:** Supervision, Software, Methodology, Investigation. **P. Fanelli:** Software, Methodology, Investigation. **E. Gajetti:** Software, Investigation. **S. Garavaglia:** Supervision, Methodology. **G. Granucci:** Supervision, Methodology. **S. Meloni:** Software, Investigation. **A. Pepato:** Supervision, Methodology. **P. Platania:** Software, Investigation. **A. Romano:** Supervision, Methodology. **A. Salvitti:** Software, Investigation. **L. Savoldi:** Supervision, Methodology. **S. Schmuck:** Software, Investigation. **M. Scungio:** Software, Investigation. **A. Simonetto:** Software, Methodology, Investigation. **M. Turcato:** Software, Investigation. **E. Vassallo:** Software, Methodology, Investigation.

Declaration of competing interest

The authors declare that they have no known competing financial interests or personal relationships that could have appeared to influence the work reported in this paper.

Data availability

Data will be made available on request.

References

[1] R. Martone, et al., Interim design report, 2019.
[2] S. Garavaglia, B. Baiocchi, A. Bruschi, D. Busi, F. Fanale, L. Figini, et al., Progress of DTT ECRH system design, Fusion Eng. Des. 168 (2021) 112678.
[3] A. Bruschi, A. Allio, F. Fanale, P. Fanelli, S. Garavaglia, F. Giorgetti, et al., Conceptual design of the DTT ECRH quasi-optical transmission line, Fusion Eng. Des. 194 (2023).
[4] F. Fanale, B. Baiocchi, A. Bruschi, D. Busi, A. Bussolan, L. Figini, et al., Progress on the conceptual design of the antennas for the DTT ECRH system, Fusion Eng. Des. 192 (2023).
[5] R.C. Wolf, et al., Plasma, Phys. Control. Fusion 61 (2019) 014037.
[6] H.P. Laqua, et al., Nucl. Fusion 61 (2021) 106005.
[7] S. Garavaglia L. Balbinot, A. Bruschi, D. Busi, A. Bussolan, F. Fanale, et al., Development of the electron cyclotron resonance heating system for Divertor Tokamak Test, J. Vac. Sci. Technol. B 41 (2023) 044201.
[8] GRASP, in: Knud Pontoppidan (Ed.), Technical Description, TICRA, 2017, (https://www.ticra.com).
[9] P.F. Goldsmith, Quasioptical Systems - Gaussian Beams Quasioptical Propagation and Applications, IEEE Press, New York, 1998.
[10] F. Leuterer, D. Wagner, J. Stober, W. Kasparek, C. Lechte, ASDEX Upgrade Team, Experimental study of Ohmic losses of polarizer mirror system, EPJ Web Conf. 149 (2017) 03002.
[11] F. Roullard, M. Bass, Transverse mode control in high gain, millimeter bore, waveguide lasers, IEEE J. Quantum Electron. 13 (10) (1977) 813–816, http://dx.doi.org/10.1109/JQE.1977.1069239.
[12] E.A. Nanni, S.K. Jawla, M.A. Shapiro, et al., Low-loss transmission lines for high-power terahertz radiation, J. Infrared Milli Terahz Waves 33 (2012) 695–714, http://dx.doi.org/10.1007/s10762-012-9870-5.
[13] A. Salvitti, Bruschi, G. Calabró, F. Fanale, P. Fanelli, S. Garavaglia, et al., Thermal and structural analyses on different mirrors of the Multi-Beam Transmission Line of DTT ECH system This Conference.
[14] A. Salvitti, A. Bruschi, G. Calabró, F. Fanale, P. Fanelli, S. Garavaglia, et al., Preliminary thermal and structural analyses on the parabolic mirror of the Multi-Beam Transmission Line of the DTT ECH system, Fusion Eng. Des. 200 (2024).
[15] K. Dutkowski, M. Kruzel, K. Rokosz, Review of the state-of-the-art uses of minimal surfaces in heat transfer, Energies (21) (2022) 7994, 2022 15, Page 7994 15.
[16] O. Al-Ketan, et al., Forced convection computational fluid dynamics analysis of architected and three-dimensional printable heat sinks based on triply periodic minimal surfaces, J. Therm. Sci. Eng. Appl. 13 (2021).
[17] E. Gajetti, M. Bonesso, A. Bruschi, F. Fanale, S. Garavaglia, G. Granucci, et al., New efficient mirror cooling for the transmission line of fusion reactor ECH systems, based on triply periodic minimal surfaces, IEEE Trans. Plasma Sci. (2023) Accepted for publication.
[18] A. Simonetto, A Small FORTRAN Program for Assessment of Alignment Tolerance in Arbitrary Sequences of Flat Or Conic Section Mirrors, Internal Report FP20/05, 2022.